

## A potential application of anodic aluminum oxide template as substrate of chemical sensors

Seo-Hyeon Jo, Sung-Gap Lee\* and Jin-Ho Yeo

Department of Ceramic Engineering, Eng. Res. Inst. Gyeongsang National University, Gyeongnam 660-701, South Korea

We fabricated the electrolyte-insulator-metal (EIM) sensor on the base of  $\text{Si}_3\text{N}_4$  film-coated AAO (anodic aluminum oxide) template for chemical sensors. The average pore size and the thickness of the AAO template were approximately 160 nm and 168 nm, respectively. The outer oxide layer thickness of the bottom part, the interface between the  $\text{Al}_2\text{O}_3$  pore and the Al metal substrate, was thicker than that of the side part, and the thickness of inner oxide layer and outer oxide layer of the bottom part were about 24 nm and 30 nm, respectively. The spacing of lattice plane of the oxide layer was about 2.387 Å. The average pH sensitivity was 51.6 mV/pH.

**Key words:** Chemical sensor, AAO.

### Introduction

Since Caras and Janata [1] introduced the concept of an ion sensitive field effect transistors (ISFETs), various biosensors based on semiconductor structures have been extensively studied [2-4]. Especially, electrolyte-insulator-semiconductor (EIS) structure, which is corresponded to the gate region of an ISFET, has considerable advantages compared to ISFET. Due to the missing photolithographic process steps, no additional passivation and encapsulation layer of the sensing area is necessary. However, since the sensitive area of an EIS sensor is in general larger than the gate region of an ISFET, more analyze is needed for a measurement. To solve this problem a new concept for potentiometric Si-based sensors has been developed using structured or porous silicon layers as transducer materials for chemical sensors and biosensors [5]. Capacitive EIS sensors based on porous Si exhibit the advantages of a produced embedment of chemical or biological recognition elements inside the pores against a fast leaching out, and the enlargement of the effective sensor area due to the pore structure.

The anodic aluminum oxide (AAO) is known for templates in fabricating nanostructures such as nanotubes, nanowires made of various materials [6, 7]. It is a self-ordered nanoporous membrane that consists of a hexagonal array of cells with uniform and parallel straight cylindrical nanopores perpendicular to the membrane surface [8]. AAO template with various surface areas can be easily made by controlling the

pore size and the interval between pores.

We presented an alternative concept based on porous metal/dielectric materials in this study. Different preparation methods have been investigated: anodic etching process of aluminum and subsequent deposition of dielectric layer of  $\text{Si}_3\text{N}_4$ , so-called EIM (electrolyte-insulator-metal) structure. And we studied the electrochemical properties for application as a transducer material for chemical sensors and biosensors.

### Experimental

Aluminum foil (99.999%, annealed, Alfa Aeser) specimens of  $1 \times 1 \text{ cm}^2$  with the thickness of 0.5 mm were prepared. AAO templates were fabricated by the two steps anodizing processes. At First, the specimens were electropolished at 20 V with  $100 \text{ mA/cm}^2$  in a mixed solution of perchloric acid and ethanol ( $\text{HClO}_4 : \text{C}_2\text{H}_5\text{OH} = 1 : 4$  in volumetric ratio) at  $10^\circ\text{C}$  for 5 min. After electropolishing, the first step of anodizing process was carried out in an oxalic acid solution for 1 h. The AAO layer was then removed by immersing the specimen in a mixture of 1.8 wt% chromic acid and 6 wt% phosphoric acid at  $65^\circ\text{C}$  for 3 h. And then porous-type AAO films were obtained by the second step of anodization carried out in an oxalic acid solution for 3 min.  $\text{Si}_3\text{N}_4$  film, which used as the sensing layer of sensor devices, was deposited by plasma enhanced chemical vapor deposition (PECVD) technique onto the porous AAO substrates. The crystalline structure of AAO templates were analyzed by X-ray diffraction (XRD) with  $\text{CuK}$  emission. The surface and cross-sectional microstructures of EIM sensors were examined using field-emission scanning electron microscopy (FE-SEM) and transmission electron microscopy (TEM). In order to examine the

\*Corresponding author:  
Tel : +82-55-772-1687  
Fax: +82-55-772-1689  
E-mail: lsgap@gnu.ac.kr

potentiometric response of the sensors, the prepared samples can be easily mounted in a home-made measuring cell sealed by an O-ring. The sensor was contacted on its front side by the electrolyte and an Ag/AgCl reference electrode, on the rear side by a gold-plated pin. To study the sensor characteristics, capacitance/voltage (C/V) measurements were performed with LCR meter (PM6306, Fluke). And for verify the potential to biosensor the voltage was investigated with various pH solution using Data acquisition/Switch unit (34970A, Agilent).

## Results and Discussion

Fig. 1 shows the XRD pattern of AAO template, in which all peaks are consistent with those of a

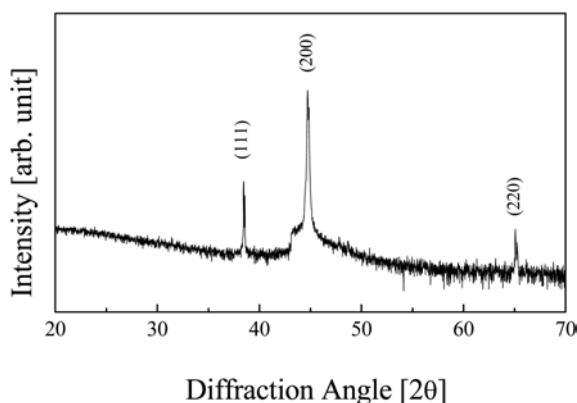


Fig. 1. XRD patterns of the anodic aluminum oxide template.

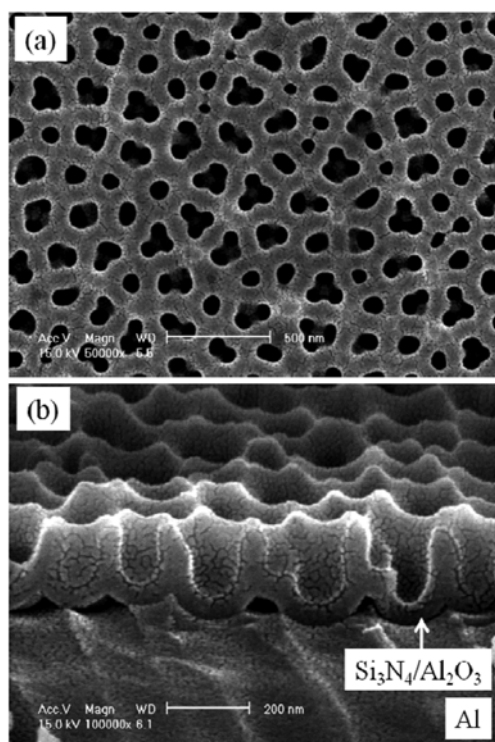


Fig. 2. (a) Surface and (b) cross-sectional FE-SEM micrographs of  $\text{Si}_3\text{N}_4$  film-coated AAO template.

polycrystalline structure  $\lambda\text{-Al}_2\text{O}_3$  (JCPDS No. 01-075-0921). The peaks in the XRD pattern are rather sharp, which indicate relatively high crystalline of the AAO template.

Fig. 2 shows the surface and cross-sectional SEM micrographs of  $\text{Si}_3\text{N}_4$  film-coated AAO template. Generally, AAO templates are fabricated with a uniform circular holes and high aspect ratio for use in preparation of the nanotube or nanowires, etc. In this work, however, we fabricated the AAO template with a large pore size and low aspect ratio for detecting the various liquid state substances as chemical sensors. As shown in Fig. 2(b), AAO template was etched with uniform thickness and funnel shape, especially, with the wider upper parts than the bottom portion. We expected that these microstructures show the excellent characteristics to detect the liquid materials due to an increase of the contact area between the electrolyte and the sensing layer. The average pore size and the thickness of the AAO template were approximately 160 nm and 168 nm, respectively.

For more detailed investigation on the microstructure of the  $\text{Si}_3\text{N}_4$  film-coated AAO template, a TEM study was performed. Fig. 3 shows a cross-sectional image of

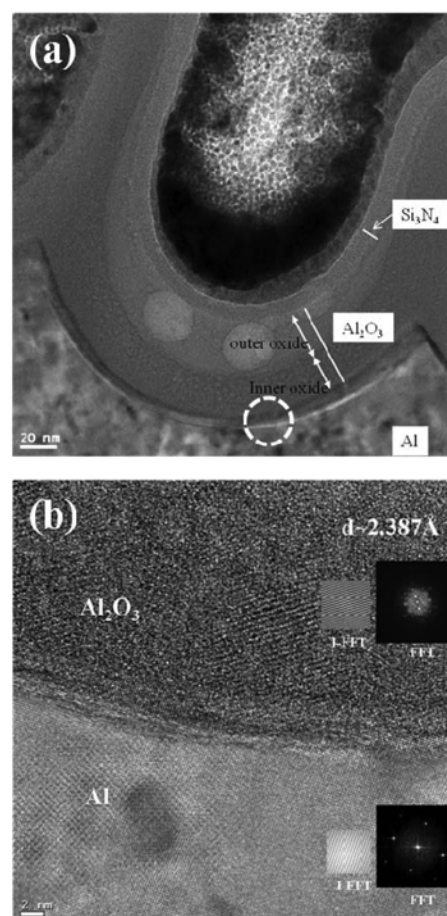


Fig. 3. (a) Cross-sectional TEM micrographs of the  $\text{Si}_3\text{N}_4$  film-coated AAO template and (b) Cross-sectional high resolution TEM micrograph of the interface between the  $\text{Al}_2\text{O}_3$  layer and Al substrate.

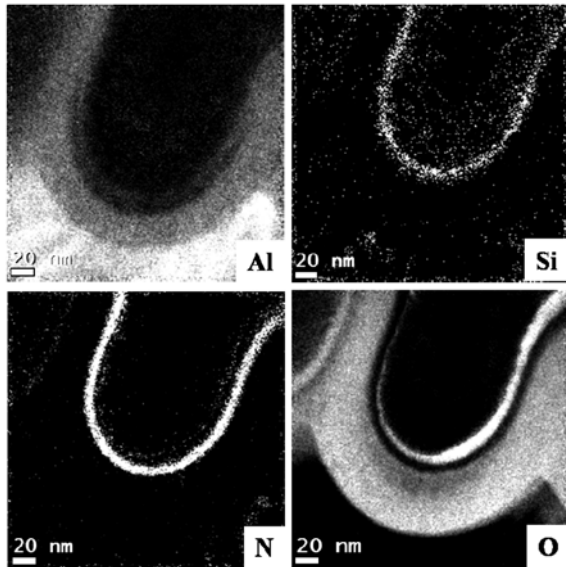


Fig. 4. TEM-EESL mapping image of  $\text{Si}_3\text{N}_4$  film-coated AAO template.

the  $\text{Si}_3\text{N}_4/\text{Al}_2\text{O}_3/\text{Al}$  interface.  $\text{Si}_3\text{N}_4$  layer was coated with uniform thickness with the thickness of about 10 nm, and pore wall as well as the pore bottom is completely covered with  $\text{Si}_3\text{N}_4/\text{Al}_2\text{O}_3$  layer sequence. Due to the porous formation of the AAO template a deposition of sensitive materials should be possible.

Generally, in the AAO process,  $\text{Al}_2\text{O}_3$  layer was composed of an inner oxide layer formed with pure alumina oxide and an outer oxide layer formed with an anion-contaminated alumina [9]. The outer oxide layer thickness of the bottom part, the interface between the  $\text{Al}_2\text{O}_3$  pore and the Al metal substrate, was thicker than that of the side part, as shown in Fig. 3(a). The thickness of inner oxide layer and outer oxide layer of the bottom part were about 24 nm and 30 nm, respectively. Fig. 3 (b) shows the selected area electron diffraction (SAED) pattern of the cross-sectional image of interface between the AAO template and the Al substrate. The appearance of spot-pattern in the diffraction pattern obtained from the oxide layer and Al substrate indicated the polycrystalline and metal phase, respectively. The spacing of lattice plane of the AAO layer was about 2.387 Å.

Fig. 4 shows the TEM-EESL (electron energy loss spectroscopy) mapping image of  $\text{Si}_3\text{N}_4$  film-coated AAO template in order to observe the formation of  $\text{Si}_3\text{N}_4$  thin film and AAO layer.  $\text{Si}_3\text{N}_4$  thin film and  $\text{Al}_2\text{O}_3$  layer having a relatively uniform thickness were formed, and the diffusion of elements at the interfaces was not observed. The thickness of  $\text{Si}_3\text{N}_4$  thin film formed by the PECVD method was approximately 9.1 nm.

In order to study the basic sensor characteristics, the sensor chip was contacted on its front side by the electrolyte and a reference electrode and on its rear

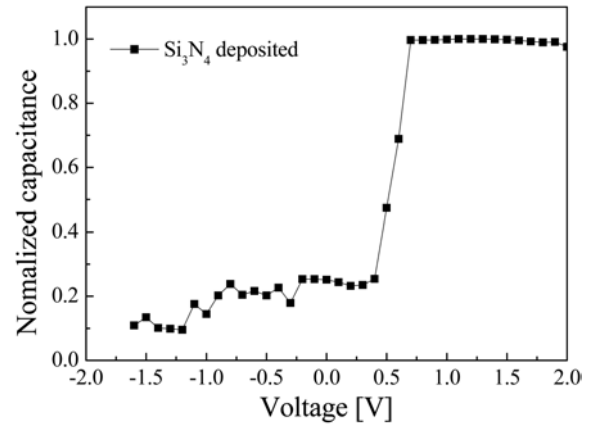


Fig. 5. Normalized capacitance-voltage property of  $\text{Si}_3\text{N}_4$  film-coated AAO template.

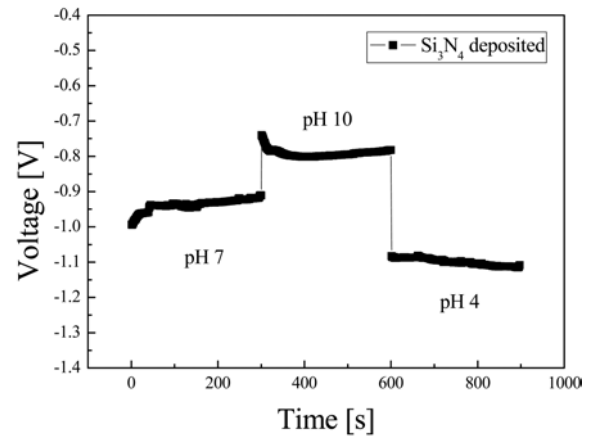


Fig. 6. Hysteresis behavior of  $\text{Si}_3\text{N}_4$  film-coated AAO template in pH 7 → 4 → 10 loop.

side by a gold-plated pin. C-V measurements were performed with a LCR meter at a dc voltage which was swept from -2 V to 2 V in steps of 100 mV and a superposed ac voltage with a frequency of 120 Hz and a signal amplitude of 50 mV. Fig. 5 shows a typical C-V curve in a working buffer (pH 8) for the porous EIM sensor with  $\text{Si}_3\text{N}_4$  layer. The set value of the capacitance (working point) was chosen from the depletion region of the C-V curve that is about 0.15 V. In this region, the curve has a linear shape, which guarantees that only the concentration-dependent potential shift as resulting chemical sensor signal is measured. The increase of the sensing area of sensors due to the porous structure raises the capacitance value of its. Since the absolute capacitance depends of the sensor area of the porous EIM structure, a proportional decrease in sensor size should be possible without any loss of the sensor characteristics.

Fig. 6 shows the hysteresis behavior for EIM sensor with  $\text{Si}_3\text{N}_4$  layer measured by immersing the prepared sensors in each pH standard solution for up to 5 min in a set cycle of pH 7 → pH 4 → pH 10. Hysteresis phenomenon can be due to the defects of an insulator film, resulting in the formation porous structures. The

interior sites of these porous defects could react with the ions existing in the tested solution and thus causes a hysteresis response. It is suggested that larger surface area should contain more slow reacting-sites. For this EIM sensor an average pH sensitivity of about 51.6 mV/pH is calculated from linear regression which is very close to the theoretical Nernstian slope of 54 mV/pH at standard conditions [10].

### Conclusions

AAO templates were fabricated by two steps anodizing processes and then deposited  $\text{Si}_3\text{N}_4$  on them by using PECVD method. The structural and electrochemical properties were observed for sensor applications as chemical sensor. AAO layer showed the typical XRD pattern of polycrystalline structure with the  $\lambda\text{-(Al}_2\text{O}_3\text{)}_{1.333}$  phase. AAO template exhibited inhomogeneous circular shape holes with a mean diameter of about 160 nm. In the pore shape of AAO template, the upper parts were wider than the bottom portion. It was expected that these microstructures has the excellent characteristics to detect the liquid materials. The pH sensitivity was about 51.6 mV/pH. These are because of the porous surface structures having slow reacting-sites.

### Acknowledgments

This research was supported by the Pioneer Research Center Program through the National Research Foundation of Korea funded by the Ministry of Education, Science and Technology (2011-0001704).

### References

1. S. Caras and J. Janata, *Anal. Chem.* 52 (1980) 1935.
2. Y. Vlasov, A. Bratov, S. Levichev and Y. Tarantov, *Sensors and Actuators B*, 4 (1991) 283.
3. H. Sakai, N. Kaneki and H. Hara, *Sensors and Actuators B*, 13-14 (1993) 578.
4. A. P. Loldatkin, D. V. Gorchkov, C. Martelet, N. Jaffrezic-Renault, *Materials Science and Engineering C5* (1997) 35.
5. M. Thust, M. J. Schoning, S. Frohnhoff, R. Arens-Fischer, P. Kords and H. Luth, *Mat. Sci. Technol.* 7 (1996) 26.
6. J. Gao, Q. Zhan, W. He, D. Sun, and Z. Cheng, *Appl. Phys. Lett.* 86 (2005) 232506.
7. K. Y. Zang, S. J. Chua, J. H. Teng, N. S. S. Ang, A. M. Yong, and S. Y. Chow, *Appl. Phys. Lett.* 92 (2008) 243126.
8. H. Masuda and K. Fukuda, *Science* 268 (1995) 1466.
9. J. Choi, Ph. D dissertation, Martin-Luther-Universität, Halle-Wittenberg, Germany (2004).
10. M. J. Schoning, F. Ronkel, M. Crott, M. Thust, J. W. Schultze, P. Kordos and H. Luth, *Electrochimica Acta* 42 (1977) 3185.